SUPERCONDUCTING CYCLOTRONS[*]

H.G. Blosser, D.A. Johnson, and R.J. Burleigh
Cyclotron Laboratory, Michigan State University, East Lansing, Mi. 48824
and R.C. Niemann and J.R. Purcell, Argonne National Laboratory, Argonne, Ill. 60439

Abstract

Superconducting cyclotrons are particularly appropriate for acceleration of heavy ions; this paper reviews design features of a superconducting cyclotron with energy 440 (Q^2/A) MeV. A strong magnetic field (4.6 tesla average) leads to small physical size (extraction radius 65 cm) and low construction costs. Operating costs are also low. The design is based on established technology (from present cyclotrons and from large bubble chambers). Two laboratories (in Chalk River, Canada and in East Lansing, Michigan) are proceeding with construction of full-scale prototype components for such cyclotrons.

1. Introduction

The idea of a superconducting cyclotron was explored at MSU in the early 60's[1] but was laid aside due to unreliability of conductors then available. In 1973 a renewed study of superconducting cyclotrons was undertaken by a group at Chalk River under Fraser.[2] After preliminary exploration Fraser's group concluded that the evolving superconducting coil technology was such that a cyclotron constructed using such a coil would be a major economic breakthru. MSU studies were reactivated in the fall of 1973[3] and at the same time studies were in progress at the Lawrence Berkeley Laboratory.[4] Both the Chalk River program and the Berkeley program are described in following contributed papers and so this paper will be devoted to discussion of results obtained in East Lansing.

Superconducting cyclotrons as presently planned combine a superconducting main coil with room temperature trim coils, rf system, vacuum tank, etc. Such a cyclotron is then fundamentally the same as present isochronous cyclotrons but with much higher magnetic fields (4-5 tesla). The superconducting main coil is similar in size and style to the coils used on a number of large bubble chambers. The oldest of these bubble chamber coils[5] has now been in service since 1969 and has proved to be extremely reliable.

The relative absence of published literature on the superconducting cyclotron means that there is much to discuss; this is in conflict with the stringent page limit for the conference proceedings. Viewing this problem I have decided to use most of the alloted space for graphic materials, so that the paper is then dominantly a collection of figures and captions,

intended to be concisely intelligible to the expert but probably difficult for the casual reader. Terminology and symbols are used without definition but in accord with normal cyclotron use (r, x, p_x, p_r, cyc. units, etc.). Proceedings of earlier cyclotron conferences are referred to for definitions.

The goals of the superconducting cyclotron program in East Lansing are at present rather general--we are trying to look at designs appropriate for a variety of different cyclotron applications, including both use as a stand-alone cyclotron and use as a post-accelerator. For the later we consider both large tandems and a preceeding cyclotron as possible first stage accelerators. In June 1975 we were authorized to proceed with construction of a full-scale prototype magnet for such a cyclotron.

2. Cyclotron Basic Structure

A coil, cryostat and refrigerator for the prototype magnet are being constructed by Argonne National Laboratory under Contract #31-109-38-3251L,[6] and will be tested at Argonne at full field before being shipped to MSU. Figure 1 is a photograph of a conductor sample and conveys the compactness of the stabilized NbTi conductor. Conductor will be wound helically on a main coil bobbin; "picket fence" spacers between layers provide 50% face cooling of the conductor via direct emersion in liquid helium. The coil bobbin after winding is welded shut and becomes the helium vessel which is in turn installed in an annular cryostat as shown in Fig. 2. The total heat leak including both radiation loss and conduction losses thru leads and support members is estimated at 5 watts.[7] Helium for the cryostat will be continuously supplied from a 500 liter storage dewar which will in turn be periodically replenished from an adjacent refrigerator (CTI Model 1400 with 2 compressors).

Two possible arrangements for the major mechanical features of the cyclotron are shown in Fig. 3 and 4. Many features of the two figures are independently interchangeable i.e., 3 sectors or 4 sectors, circular yoke or "cross" yoke, forgings or plates for the yoke, single dee stems or double dee stems, etc. The small insert in Fig. 3 shows a central region layout for a stand-alone cyclotron. For this configuration the central hole in the magnet is filled by iron plugs, the dees extend to the center and multiple ion sources, used one at a time, inject particles into one or the other of the 3 dees in the fashion of the Karlsruhe cyclotron.

Fig. 5 shows details of a possible pole tip geometry and the calculated magnetic field for this geometry. The calculations use the "uniform magnetization" approximation[8] with a saturation field strength of 2.0 tesla. In two dimensions, calculations of this type agree quite accurately with relaxation calculations at the field levels relevant here (fully saturated iron). We assume such calculations to be similarly reliable in three dimensional azimuthal varying structures such as will be involved in the cyclotron.

The data in Fig. 5 are specifically for a four sector field. (The nature of the calculation is such that the average field does not depend on the number of sectors providing the fractional sector width is kept the same.) Generally in our studies we are looking at both three and four sector geometries but most of the results presented herein are for the four sector field. Computations for three sectors are not as far advanced but are being worked on extensively. (Weighing relative advantages of the two choices as known at this time tends to favor the three sector geometry.)

The magnet calculations include computing the field for a set of trim coils with geometry as in Fig. 3 and then using these trim coils in a fitting program to produce isochronous average fields. Fig. 5 shows a typical result for such a fitted field compared with the isochronous field and Table 1 gives results for trim coil power from a number of calculations of this kind.

As described previously,[8] fields such as considered here are characterized by both a bending limit and a focussing limit. These limits are plotted for the four sector field in Fig. 6. The focussing limit for the three sector field is approximately 10% higher.

The orbital frequency, the magnetic field, the turn number and the turn number times harmonic number are given in Fig. 7 versus Q/A. (The ion is assumed to be running at it's maximum energy with the dees operating at their full 100 kV level.) Curves are presented for both three sector and four sector rf systems. Over the interesting range of Q/A (~1/6) the turn number is substantially lower than in the present generation of cyclotrons and single turn extraction should therefore be feasible even with the somewhat more diffuse beams expected for heavy ions. (For a stand alone cyclotron we would break the turn number graph into a set of fixed orbit geometry groups whereas a booster would be operated at full voltage at all times.)

Figs. 8, 9 and 10 show results of acceleration studies[1] in the design field (the "all dees in phase" curve of Fig. 7) and 2) with a variety of errors, i.e. 1 dee phase shifted by 5°, a +5% voltage error in the rf system and the outer magnetic ring (the inner cryostat wall) displaced by 0.8 mm. The design is relatively insensitive to such errors which is primarily a consequence of the matching symmetry of the rf system and magnet.

3. Injection

When the cyclotron is used as a booster accelerator, injection and capture are accomplished by change of charge state in an internal stripping foil. The beam from the previous accelerator must then be sufficiently rigid to push its way into the magnetic field of the booster and beyond the center so as to match smoothly to a closed orbit after the charge change. This leads to an "injection limit" on the energy gain of the booster--for a hard-edge, azimuthally symmetric magnetic field this limit is given by:

$$E_f/E_i < (1 - 2Q_f/Q_i)^2 \qquad (1)$$

The behavior of such a system can be inferred using the approximate formula of Betz[9] to estimate the charge after stripping. Curves of $\bar{Q}$ vs E/A obtained in this way are given in Fig. 11. A helpful feature of the stripping process is the approximate $\sqrt{E/A}$ dependance which means that rigidity $B\rho (=p/\bar{Q})$ after stripping is rather independant of energy.

A further requirement on the injection system is that ions enter from a reasonably convenient beam transport system, i.e. preferably that injection trajectories come from a single common steering magnet at the outside of the cyclotron. Also, the internal stripping foil must be well away from acclerating gaps. To determine the injection line location a survey of all possible foil locations is useful and is shown in Fig. 12. A fixed vertical line in this figure shows the azimuthal range of required entry points in order to hit a foil at a fixed angular location. A horizontal line in the figure shows the range of foil location angles needed to match a single external entry point. The sense of the magnet spiral has great influence on these contours ("along the spiral" is illustrated by the arrangement in Fig. 3--"against the spiral" by the arrangement in Fig. 4).

The Fig. 12 data imply foil locations too close to the accelerating gap when a single external entry point is assumed; two entry points were therefore introduced which then group the injection paths as shown in Fig. 13 when injecting from a 25 MV tandem. (For light ions charge states are assumed to be reduced to lower than

equilibrium values in the tandem terminal by lowering the gas pressure in the stripping cell, a process which has been experimentally tested at Chalk River.[10]) Fig. 14 is an expanded view of the family of foil locations from Fig. 13 and establishes the range over which the foil positioning mechanism must operate. Fig. 15 is similar to Fig. 13 except with an assumed 13 MV tandem as the injector. The striking similarity of Figs. 13 and 15 reflects the constant rigidity character of the stripping curves in Fig. 11. When the previous accelerator is assumed to be a cyclotron the family of injection orbits is much more homogeneous than indicated in Figs. 13 and 15 since frequency matching of the cyclotrons requires that injection always go to the same radius equilibrium orbit irrespective of what ion is injected.

Fig. 16 shows the optical characteristics of the injection path. The calculation was set up to find the phase elipse at the field edge which would focus to a 2 mm diameter circle at the stripping foil. The required elipse is seen to be compact and linear. In addition an energy shift would have essentially no affect on the process if the injection line is dispersion-matched. Runs with an axial ellipse give an even more compact phase space figure (7 mm in transverse width at the field edge).

A crucial element in the stripping injection system is a foil magazine and a foil insertion mechanism. We have worked out a design for a foil magazine[11]) which mounts along the magnet axis with insertion of new magazines thru a vacuum lock from the top and with a slide-projector-like mechanism at the bottom to pick foils from the magazine and place them in any of the Fig. 14 locations. Some details of this mechanism are shown in Fig. 17. Used foil frames fall to the bottom of the cyclotron and must be occasionally removed, again through a vacuum lock. From existing data on foil lifetimes it appears that this mechanism will be totally adequate.

4. Extraction Studies

Extraction from a superconducting cyclotron is inherently difficult as a consequence of the strong magnetic field. A major criteria in arranging the basic coil and iron geometry is then to provide a sharp edge on the field so as to facilitate extraction. With reasonable steps, field edges such as indicated in Fig. 5 can be achieved and extraction can then be accomplished with a variety of devices. A survey of a number of likely devices is shown in Fig. 18 which is a polar map of central rays. The weakest workable system (more-or-less) is a pair of electrostatic deflectors operating at a 140 KV/cm. The strongest is an electrostatic deflector

followed by a superconducting magnetic shield which gives B=0 in the internal region of the shield.[12]) The several systems in Fig. 18 lead to a major difference in beam quality as a result of the very different path lengths in the fringe field. This is shown in Fig. 19 which shows the radial phase space distribution at the field edge from a 2 mm diameter circle at the deflector entrance. The two electrostatic deflectors give a very broad distorted beam profile which would be essentially impossible to refocus in a later optical system. The superconducting shield tube on the other hand leads to a fine pencil like beam with excellent optical properties. The several intermediate devices are based on a magnetic channel identical to the present MSU channel for the weakest and with scaling of this device for the two stronger cases. The strongest of these is clearly the most attractive on beam optics and is based on a doubling of the current and a halving of the scale parameter of our present channel (which can only be accomplished with superconducting windings). Our first choice extraction system is then the superconducting shield--if difficulties develop in this we will shift to an active superconducting coil designed to yield the 1.6 tesla, 1.0 tesla/inch parameters.

To obtain more experience with superconducting shield tubes we are at present in the process of installing such a tube in one of our existing beam transport system magnets so as to explore alignment techniques, beam protection, etc. A superconducting shield tube has been loaned to us by Stanford for this purpose--this tube is shown in Fig. 20.

5. System Performance

Fig. 21 shows the energy per nucleon vs. mass number when the superconducting cyclotron is used as a post-accelerator for either a 13 MV or 25 MV tandem. Foil stripping is assumed in all cases at the cyclotron injection point and curves are given for both foil and gas stripping in the tandem terminal. Note that foil stripping in the tandem terminal is advantageous only for large values of A--for small A, foil stripping in the tandem gives too high a charge state and total system performance is then limited by injection per Eq. (1). At very small values of A, the gas cell also gives too high a charge--cell pressure must then be reduced to maximize the intensity of the desired sub-equilibrium charge state. With either tandem, the energy per nucleon is seen to be well above the Coulomb barrier and a broad spectrum of important research topics is open for exploration.

Injection from a preceeding cyclotron is basically more complicated due to the

need for synchronous operation of the rf systems in the two cyclotrons. An immediate result of the synchronism requirement is that the second cyclotron must always function as an energy multiplier with the multiplication being determined by the ratio of harmonic numbers and radii, i.e.

$$E_2/E_1 = (h_1/h_2)^2 (r_2/r_1)^2 \qquad (2)$$

(assuming that both cyclotrons operate with the same rf frequency so that all "buckets" are filled). It then immediately follows from (2) that the final energy E_2 is given by

$$E_2/A = (h_1/h_2)^2 (r_2/r_1)^2 K_1(Q_1/A)^2 \quad (3)$$

Note that the Q and K in the second cyclotron do not appear in (3). Rather they are fixed by the separate condition

$$K_2(Q_2)^2 = (h_1/h_2)^2 K_1(Q_1)^2 \qquad (4)$$

If this condition can be satisfied with $Q_2 = \bar{Q}$, operation can be at maximum intensity. This might however require K_2 greater than the maximum K_2 which is not possible. Q_2 must therefore exceed $\bar{Q}$ and it is then necessary to pick Q_2 in the fringe of the stripping distribution at the expense of reduced intensity. These factors are graphically illustrated in Fig. 22 which includes in each section two sets of curves, one giving the maximum energy per nucleon per Eq. (3) and the other set indicating the intensity loss where operation off of peak charge is necessary.

At the left in Fig. 22 are curves for a pair of identical 440 MeV cyclotrons with harmonic ratio of 4. The maximum energy curves for present source technology (charges 6 or 8) fall mostly in the peak intensity region. However if one looks forward to future source improvements (charge 10 or 12) the curves fall in the reduced intensity region and performance would be severely hampered. A larger first cyclotron such as indicated in the middle section of the figure substantially alleviates the problem or shifting to a harmonic ratio of three (the right hand curves in Fig. 22) also alleviates the problem although at the expense of reduced energy for a given initial charge state.

5. Conclusion

The superconducting cyclotron is a compact economical device for accelerating heavy ions. Adequate solutions to all design problems seem to be available. This will be confirmed as construction projects move forward.

6. References

1. R.E. Berg, Magnetic Coil Design for a Superconducting Air-cored 40 MeV Cyclotron, MSU report MSUCP-14(1963).

2. C.B. Bigham, J.S. Fraser, and H.R. Schneider, Superconducting Heavy Ion Cyclotron, CRNL report AECL-4654(1973).

3. H.G. Blosser, Proceedings of Quebec Heavy-Ion Accelerator Symposium, McGill Univ. (1973).

4. D.J. Clark, Proceedings of Quebec Heavy-Ion Accelerator Symposium, McGill Univ. (1973).

5. J. Purcell, Superconducting Magnet System for the 12 foot Bubble Chamber, Argonne report ANL/HEP 6813(1968).

6. R. Niemann, Project Manager; J. Purcell, Responsible Scientist.

7. J. Purcell (private communication).

8. H.G. Blosser and D.A. Johnson, Nucl. Inst. and Meth. 121,301(1974).

9. H.D. Betz, Rev. Mod. Phys. 44,465(1972).

10. J. Ormrod (private communication).

11. Mechanical design by R.J. Burleigh, 2828 Prince St., Berkeley, California.

12. F. Martin, S.J. St.Lorant and W.T. Toner, Nuc. Inst. Meth. 103,503(1972).
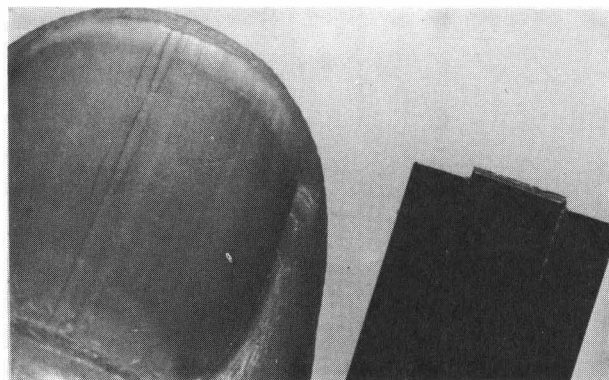
Fig. 1.--Sample 1000 ampere main coil conductor. Cu stabilization bar 1.5 mm thick x 9 mm wide. NbTi filaments in 0.8 mm x 4 mm insert.
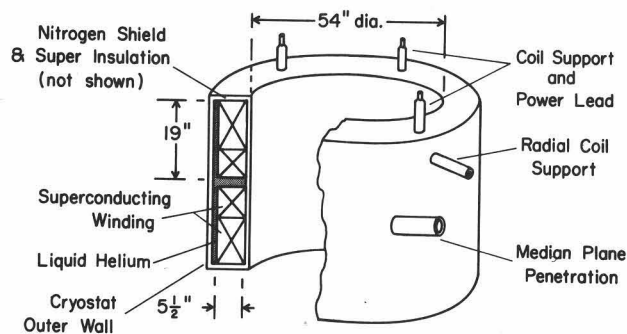

Fig. 2.--Schematic diagram of the superconducting coil and cryostat. Winding active area has 60" inner diameter and ±1.5" spacing from median plane. Amp-turns=2x(2,360,000).
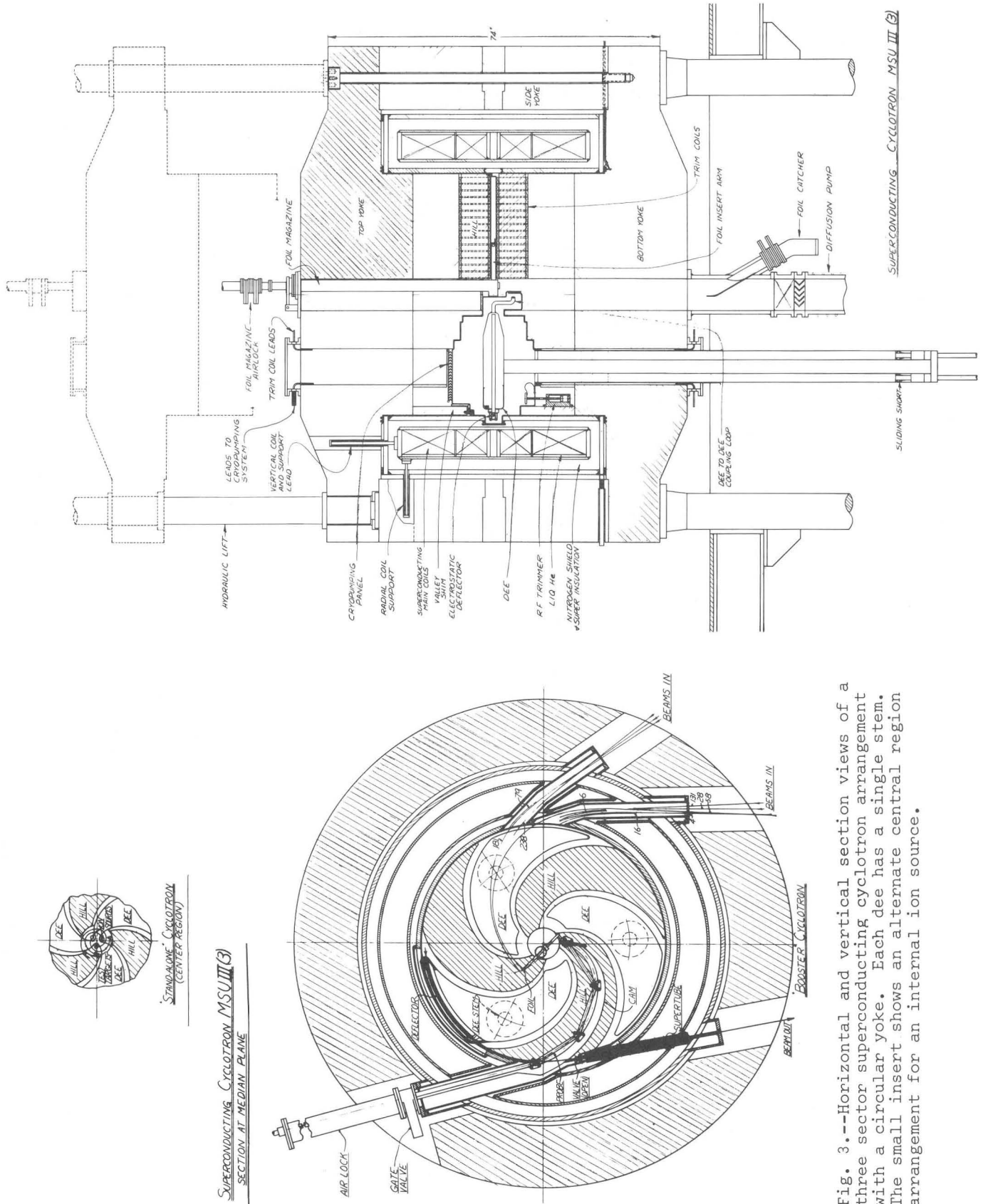
Fig. 3.—Horizontal and vertical section views of a three sector superconducting cyclotron arrangement with a circular yoke. Each dee has a single stem. The small insert shows an alternate central region arrangement for an internal ion source.
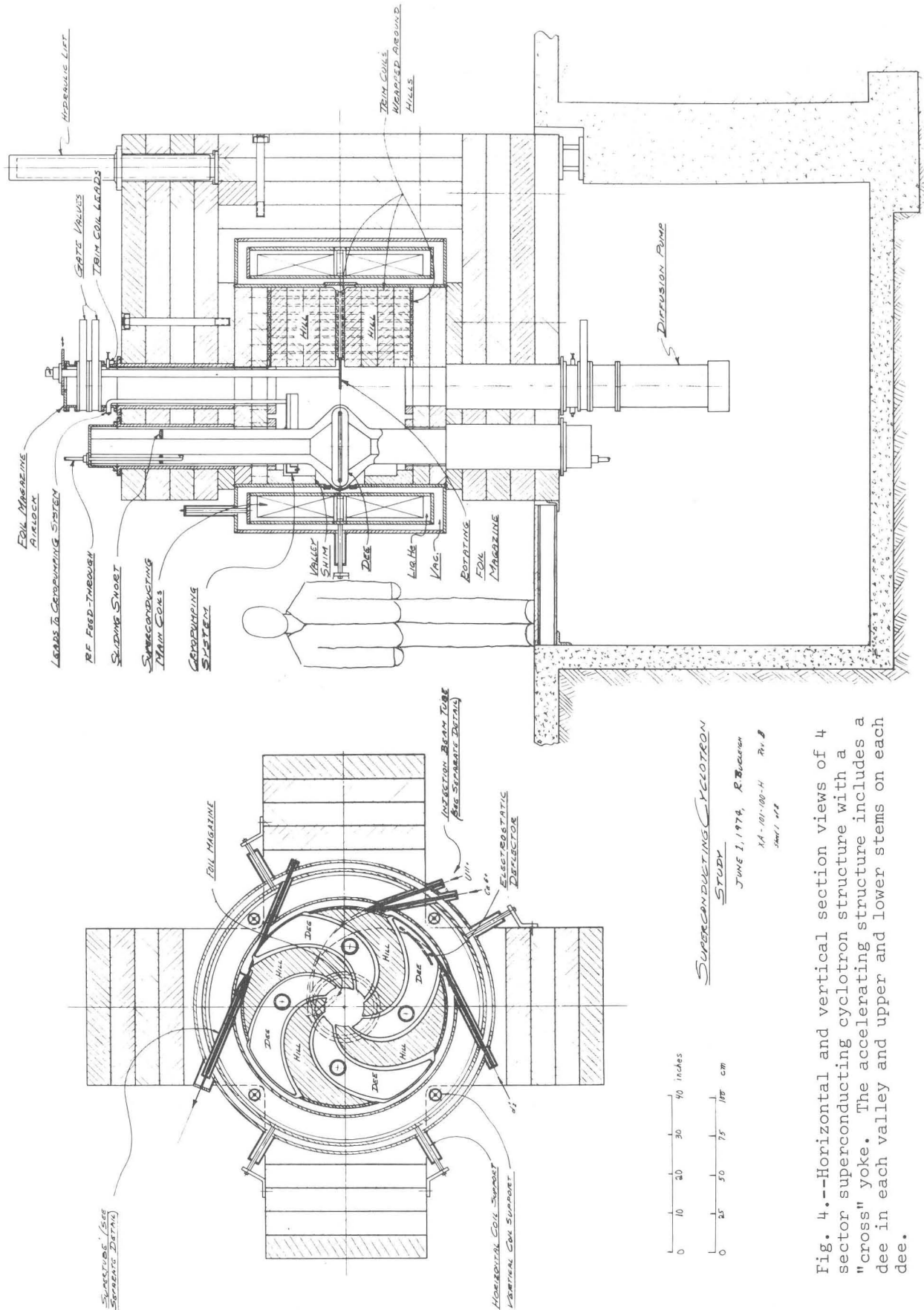
Fig. 4.--Horizontal and vertical section views of 4 sector superconducting cyclotron structure with a "cross" yoke. The accelerating structure includes a dee in each valley and upper and lower stems on each dee.
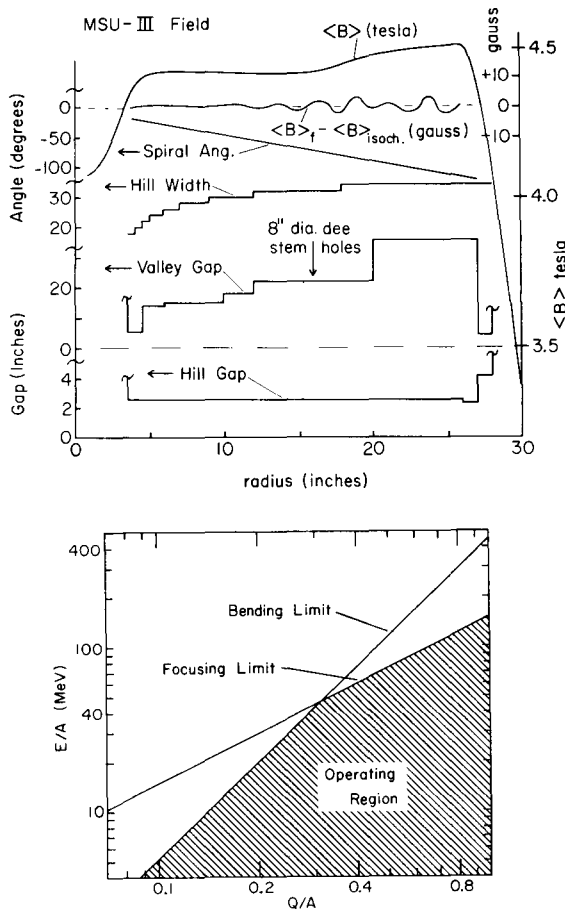
Fig. 6.--Bending limit and focussing limit for the MSU-III field. (See ref. 8 for discussion of limiting phenomena.)
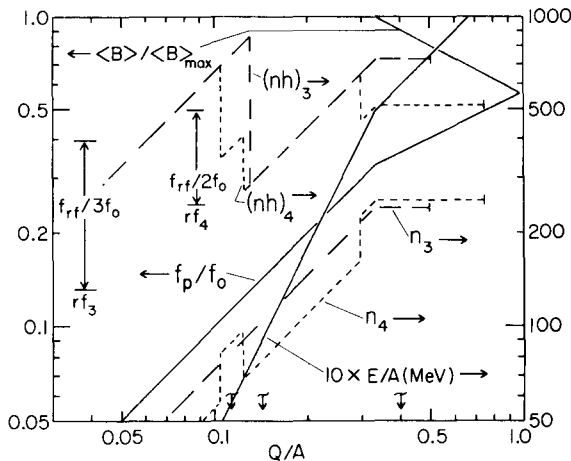
Fig. 7.--Maximum energy/nucleon vs. ion Q/A. (repeat of Fig. 6). Also magnetic field and particle orbital frequency f_p at maximum energy (f_o is freq. for Q/A=1 and $<B>_{max}$.). Also number of turns, n, and product with harmonic number, nh, for rf systems of Fig. 3 & 4 with 100 kV per dee.

Fig. 5(left).--Lower four curves--pole tip shape used for calculation of MSU-III field (4 sectors). Main coil per Fig. 2. Upper curve--magnetic field from coil and iron computed assuming $\tilde{M}_S = \tilde{k}M_O$ and saturation field strength of 2.0 tesla (see ref. 8). Next to top curve--result of fitting calculation with trim coils as in Fig. 3.
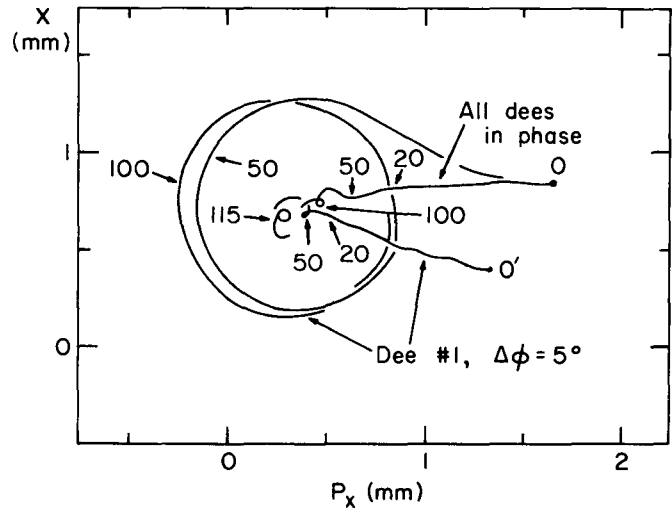
Fig. 8.--Displacement from closed orbit for particle accelerated by spiral dees in MSU-III field. "Dees in phase" curve-- precession effects are small. Phase error (5°) on one dee gives precession amplitude of 0.5 mm if starting position unchanged. Corrected by shift to starting position 0' as indicated. Integers give turn number.
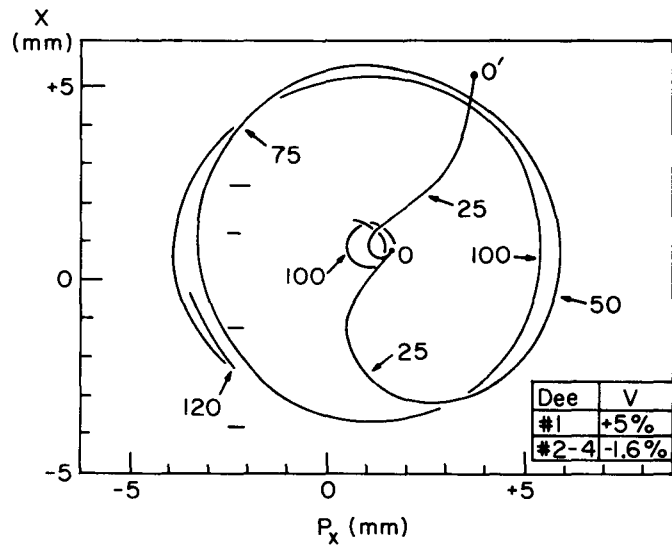

Fig. 9.--Same as Fig. 8 but with one dee raised in voltage (5%) and others lowered (1.6%). Precession amplitude of 4 mm is induced. Corrected to 0.5 mm by shift to starting position 0'.

TABLE I.--Trim coil power (total) for various ions and field levels.

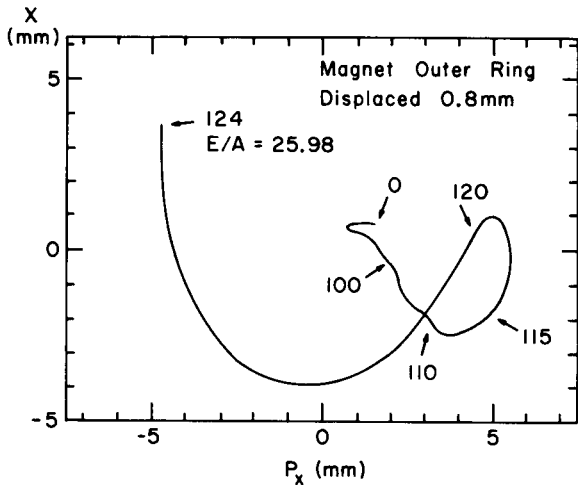| Q/A	$\langle B\rangle/\langle B\rangle_{max}$	kw
1/10	1	64.2
1/10	0.58	98.5
1/4	1	20.3
1/2	0.82	133.0
1/2	0.75	110.7

Fig. 10.--Same as Fig. 8 but with the 1" thick inner wall of cryostat displaced 0.8 mm. Precessional amplitude of 5 mm is induced at $Q_r=1$. This can be corrected by harmonic coils or by careful centering of the cryostat wall. Shifting the main coil produces a similar result.
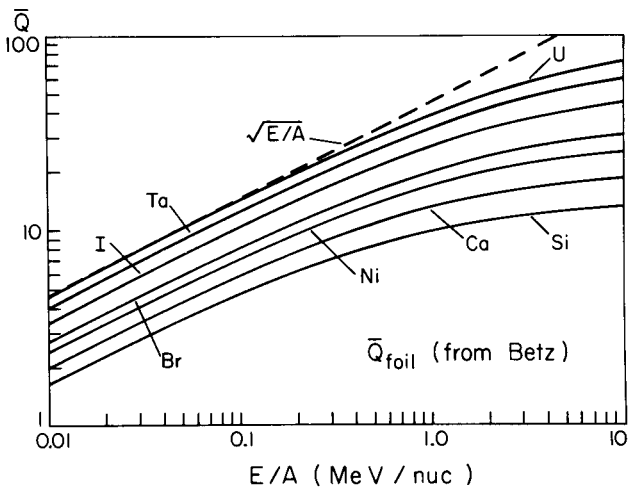
Fig. 11.--Equilibrium charge from stripping foil for various elements vs. energy. The dashed $\sqrt{E/A}$ line corresponds to constant magnetic rigidity after stripping.
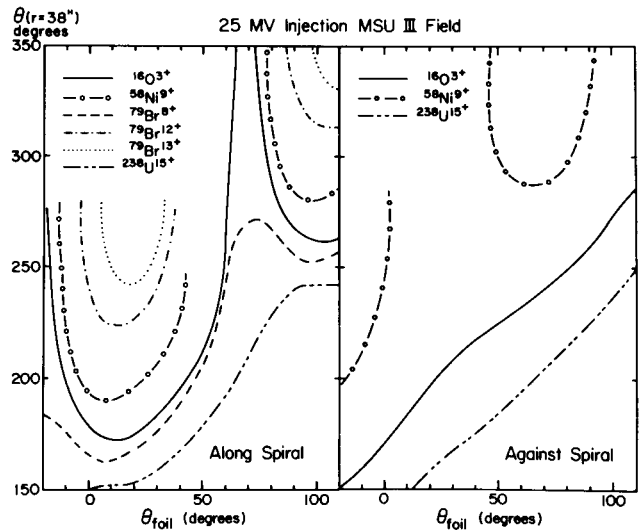
Fig. 12.--Azimuth at which injected ions enter magnetic field vs. stripping foil azimuth. Stripping foil on closed orbit for most probable after-stripping charge and injection orbit tangential to closed orbit, i.e. After stripping $x=p_x=0$ for most probable charge. Energy=(Q+1)x25 MV. Against spiral $^{79}Br^{12+}$ etc. not captured.
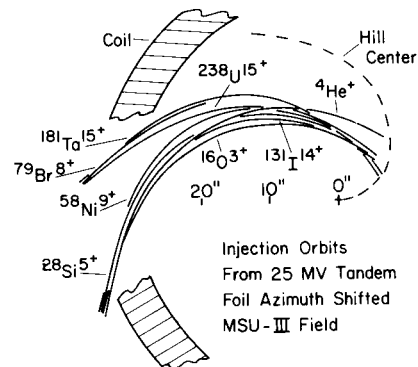

Fig. 13.--Polar plot of injection orbits for a variety of ions from a 25 MV tandem. The foil azimuth has been shifted to group the accelerated particles into two injected beam lines. After-stripping $x=p_x=0$.
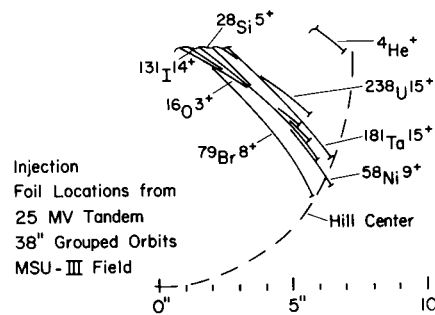

Fig. 14.--Expanded view of foil locations for orbits shown in Fig. 13. (Further optimization would group the foil locations symmetrically about the hill center.)
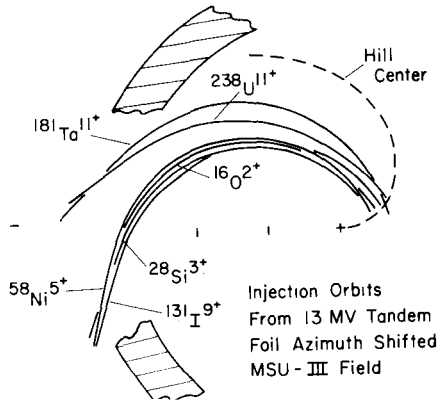
Fig. 15.--Injection scan as in Fig. 13 but with charge states and energies corresponding to 13 MV tandem.
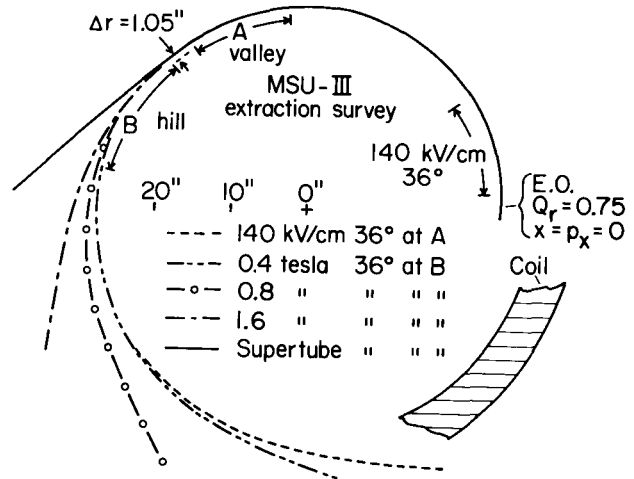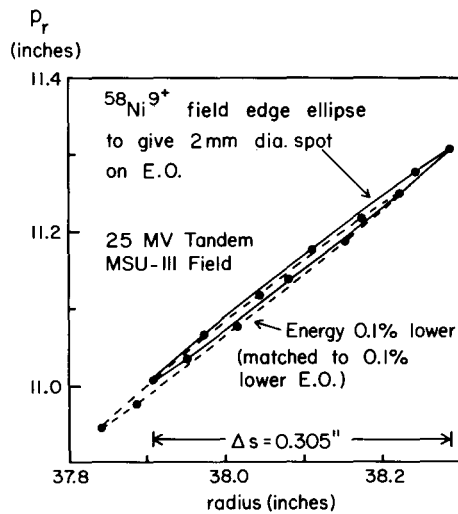

Fig. 16.--Radial phase space around one of the orbits from Fig. 13. The area shown focusses to 2 mm diameter circle (cyc. units) at the foil. The dashed curve shows a similar group with energy shifted by 0.1% and shows that dispersion matching on the injection path will be easy to accomplish.

Fig. 18.--Survey of possible extraction systems for four sector MSU--III field. All systems have initial 140 kV/cm electrostatic deflector located in a valley and five different options for a following electrostatic or magnetic device as indicated by the coded curves.
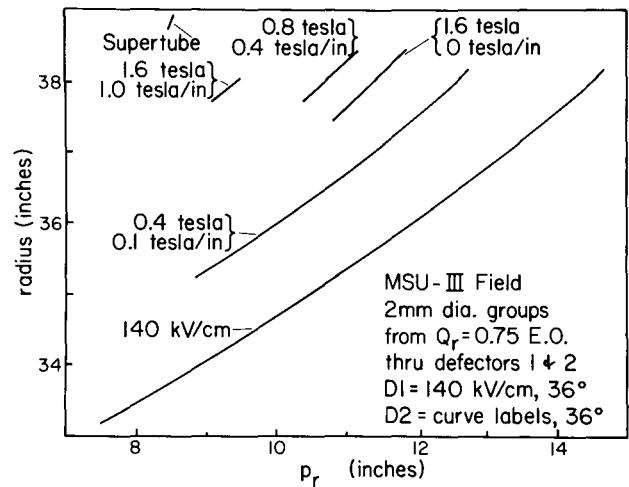

Fig. 19.--Radial phase space distribution after passing through the extraction systems of Fig. 18 (initial conditions are 2 mm diameter circle).
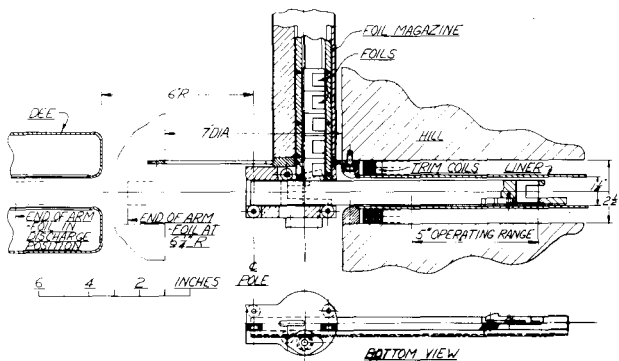
Fig. 17(left).--Mechanical drawing showing details of the vertical stripping foil magazine and horizontal foil insertion arm. Foils can be positioned over the full range shown in Fig. 14. Foils are inserted in 50 foil magazines thru a vacuum lock.
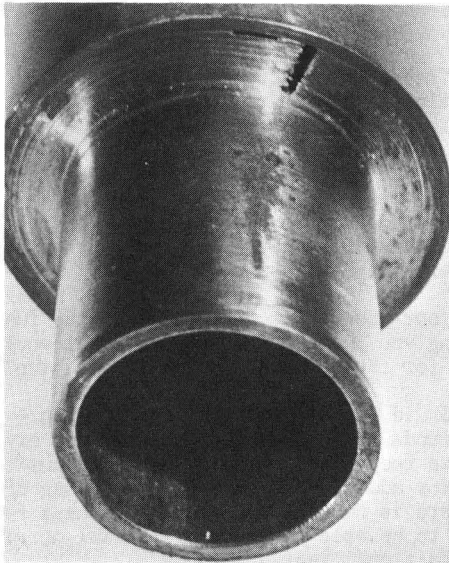
Fig. 20.--View of super tube test section on loan from St. Lorant of SLAC. Shield consists of multiple 50 μm layers of Nb³Sn. Beam tube has 16 mm clear inner bore. Shielding tested to 4.5 tesla--being prepared for beam interaction test.
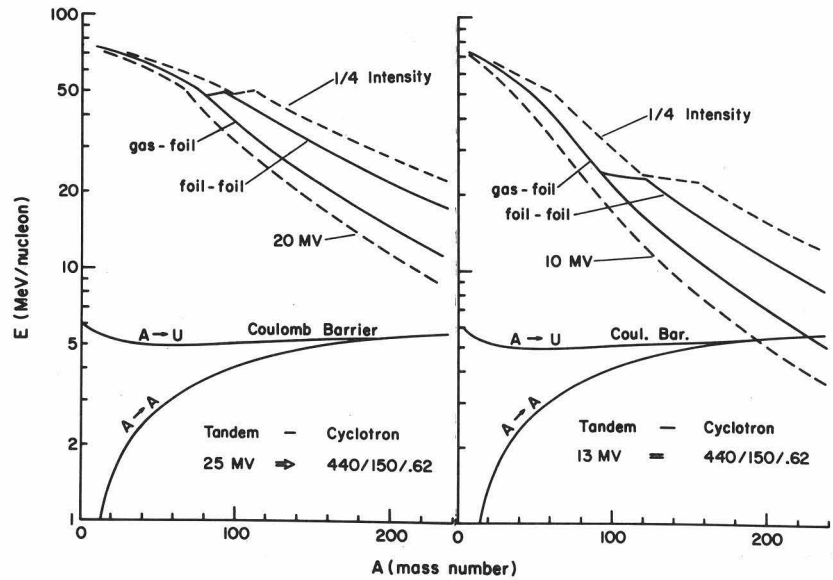

Fig. 21.--Energy per nucleon vs. mass number for accelerator systems consisting of 25 MV or 13 MV tandem plus superconducting cyclotron. Solid curves assume most probable charge in tandem terminal and at cyclotron injection and include focussing limits and injection limits (sub-equilibrium charge states are allowed in the tandem terminal when gas stripping is used). Lower dashed curve--conservative (reduced tandem voltage). Upper dashed curve--energy if operation is at the half intensity point on the stripping distribution in both tandem terminal and cyclotron (giving total intensity reduction of x4).
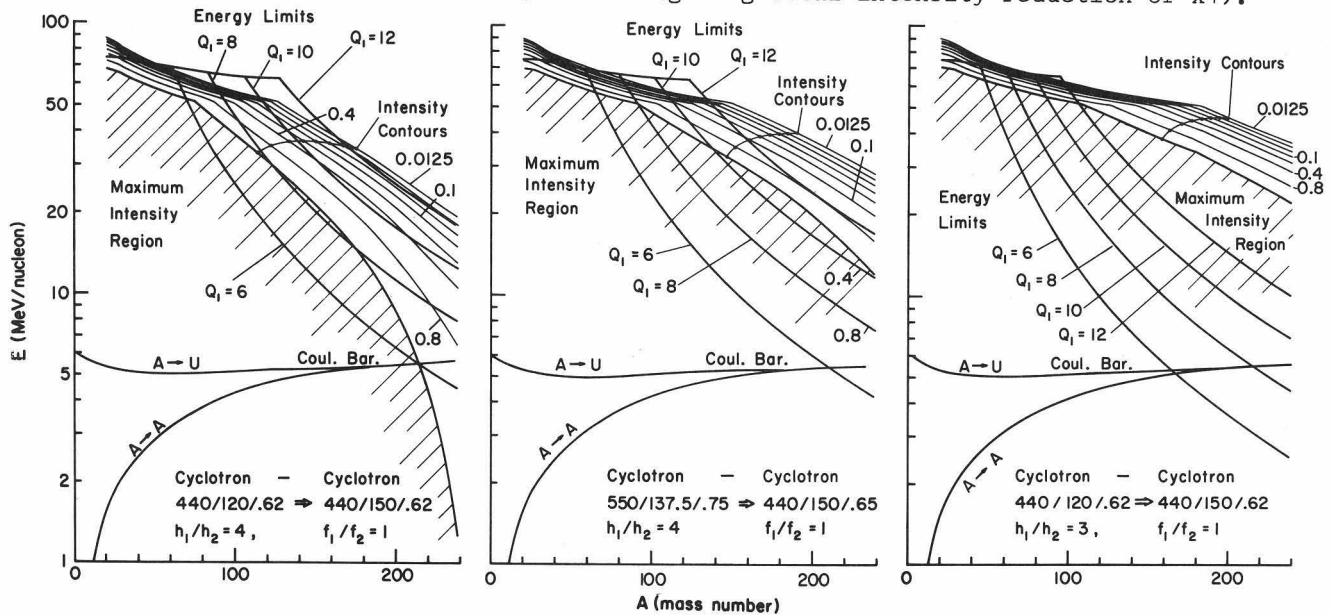

Fig. 22.--Energy/nucleon vs. mass number for cyclotron-cyclotron systems. Cyclotrons designated by bending limit and focussing limit in MeV and radius in meters, i.e. 440/150/.62. Locked rf systems (with frequency ratio and harmonic ratio as shown) gives energy limit fixed entirely by the charge state in the first cyclotron labeled $Q_1=6$, etc. When the charge state needed in the second cyclotron exceeds the most probable charge, operation is at reduced intensity as indicated by the contours .8, .4, etc. Equal cyclotrons with harmonic ratio of 4 (left) do well with present charge states ($Q_1=6-8$) but likely source improvements ($Q_1=10-12$) lie dominantly in the reduced intensity region. This problem is cured by a larger first cyclotron (center) or by changing harmonic ratio to 3(right).

DISCUSSION

M. REISER: Are you using trim coils to get iso-chronism?

H.G. BLOSSER: Yes, there are 15 coils on each hill. Simply, room temperature windings wrapped around the upper third of each hill as shown in Fig. 3 of the paper. The total power -- the sum for all coils -- stays below 100 kW.

J.R. RICHARDSON: What will be the distance between turns at extraction and what will be the amplitude of radial oscillation corresponding to the expected emittance?

H.G. BLOSSER: The number of turns varies with Q/A. For a typical value (100 turns) the natural separation is 3 mm. We would in any case use precessional extraction beyond $Q_r = 1$ and have a radius gain of about 7 mm as in our present cyclotron. Emittance data from a central ion source is as far as I know not available for very heavy ions. Emittance data from tandem beams is available and the 2 mm diameter phase space circle which we use is based on this data including multiple scattering in the stripping foil.

G. SCHATZ: Your supertube should have a strong stray field outside. What are you going to do about this?

H.G. BLOSSER: The dipole moment is in fact less than for other magnetic channels because the current distribution is the most compact possible distribution. Nevertheless this dipole moment will have to be compensated. We have not yet as looked at detailed solutions. A trivial solution is to put a supertube in each sector but I doubt that that is the best solution.

R.J. SLOBODRIAN: As I understand, you have room temperature coils in addition to the superconducting coil. Are you going to get the fine stabilization of the magnetic field using the room temperature coils or the superconducting coils or both?

H.G. BLOSSER: Superconducting coils of the type used here are completely stable in the cryogenic sense. If a section of the superconductor goes normal the current simply shifts into the adjacent copper and a small voltage drop appears, but the magnetic field remains the same depending only on the current regulation of the power supply as in conventional room temperature coils. It is a very different situation from synchrotron magnets where the pulsing tends to cause wires to move giving flux jumps and other instabilities.

J.S.C. MCKEE: You mentioned that the capital cost of the superconducting cyclotron was likely to be around 50% of that for a conventional isochronous cyclotron of the same energy. Would you care to comment on the recurrent expenditure involved in the operation of both machines, bearing in mind helium losses and their different power requirements?

H.G. BLOSSER: The superconducting cylcotron should also be substantially cheaper to operate. The refrigerator for the machine I described has a 50 horse-power motor which operates on an approximate 25% duty cycle. This is much less than the magnet power in any conventional cyclotron that I know of. The RF power is also less because of the small size of the "Dees". We calculate 18 kW per "Dee" and so the total RF power will certainly be less then 100 kW.

G. DUTTO: I do not know about the status of the funding, but assuming you receive the funding, what would be the schedule for the construction of the machine?

H.G. BLOSSER: I did mean to speak of the funding -- we do now have funds to construct the magnet and expect this to take two years. We will soon be submitting a request for additional funds to provide an RF system -- if there is no delay in receiving these funds we would expect to be able to have first trial operation after an additional year.

Y. JONGEN: What do you think about the use of the supertube as a general device for extraction in any cyclotron?

H.G. BLOSSER: We studied this problem for our MSU cyclotron and in one respect it was very attractive, namely the savings in electrical power would, at present rates, equal the capital cost of the supertube conversion in about six years. We have turned away from the idea, however, because of difficulty in exactly matching to our present beam transport system. The fact that the supertube has a different ratio of bending effect to focusing effect makes it not possible to exactly match simply by installing a tube. The easiest matching solution seemed to be to rotate the cyclotron by 20° but in the end we decided this was too difficult. We are also heavily occupied by the new project.

T. KUO: You described in your abstract that extraction is a potential problem due to high field. Can you discuss a little bit about your extraction system? What is the potential to be used in your deflector?

H.G. BLOSSER: This is discussed in the paper. 140 kV/cm is needed in the electrostatic deflector. This gives one inch of turn separation at the entrance to the magnetic channel. (The 140 kV/cm was adjusted to obtain the one inch.)